*Microenvironment and Immunology*

# Effects of Acute versus Chronic Hypoxia on DNA Damage Responses and Genomic Instability

Isabel M. Pires[1], Zuzana Bencokova[1], Manuela Milani[2], Lisa K. Folkes[1], Ji-Liang Li[2], Mike R. Stratford[1], Adrian L. Harris[2], and Ester M. Hammond[1]

## Abstract

Questions exist concerning the effects of acute versus chronic hypoxic conditions on DNA replication and genomic stability that may influence tumorigenesis. Severe hypoxia causes replication arrest independent of S-phase checkpoint, DNA damage response, or transformation status. Arrests occur during both the initiation and elongation phases of DNA replication, correlated with a rapid decrease in available deoxynucleotide triphosphates. With fluctuating oxygen tensions in tumors, arrested hypoxic cells may undergo rapid reperfusion and reoxygenation that leads to reoxygenation-induced DNA damage. In cells subjected to chronic hypoxia, we found that replicative restart was inhibited along with numerous replication factors, including MCM6 and RPA, the latter of which limits the hypoxia-induced DNA damage response. In contrast, in cells where replicative restart occurred, it was accompanied by extensive reoxygenation-induced DNA damage and compromised DNA repair. We found that cells reoxygenated after acute hypoxia underwent rapid p53-dependent apoptosis. Our findings suggest that cells lacking functional p53 are more susceptible to genomic instability and potentially tumorigenesis if they experience reoxygenation after acute exposure to hypoxia. *Cancer Res; 70(3); 925–35. ©2010 AACR.*

## Introduction

Regions of hypoxia occur in all solid tumors as a result of an abnormally formed tumor vasculature and inadequate perfusion of the tumor mass. The occurrence of regions of low oxygen is an indicator of poor patient prognosis due to increased chemo- and radio-resistance, genomic instability, and metastatic potential (1, 2). The occurrence of episodes of reoxygenation following hypoxic exposures of various degrees is inherent to the dynamic nature of the tumor vasculature (3, 4). The range of oxygen tensions within a tumor varies between approximately 8% and 0.02% (near anoxia, 100–150 μm from blood vessels; ref. 5). Previous reports showed that severe hypoxia ($p$O$_2$ <0.02%) induces an S-phase arrest due to inhibition of DNA synthesis in a HIF-1–independent manner (6, 7). Hypoxia-induced replication stress was shown to induce activation of the DNA damage response (DDR) apical

kinases ataxia telangiectasia mutated (ATM) and ATM-related (ATR) and phosphorylation of downstream targets such as p53, Chk1, and Chk2, albeit in the absence of detectable DNA damage (6, 8, 9). In contrast, reoxygenation was shown to rapidly induce DNA damage and, consequently, a more conventional Chk2-dependent DDR leading to a G$_2$-M arrest (10, 11). Replicative stress and the subsequent induction of the DDR occur early in tumorigenesis and have been proposed to act as a barrier to tumor progression (12, 13). It has been suggested that hypoxia could contribute to this because hypoxic regions can form in preneoplastic lesions (13, 14).

In this study, we have characterized the hypoxia-induced S-phase arrest, showing that, at the molecular level, it is associated with an inhibition of DNA replication in both the initiation and elongation phases. Chronic hypoxia exposure actively induces disassembly of the replisome, preventing replication restart after reoxygenation. However, acutely exposed cells are still able to restart replication despite the presence of an active checkpoint response and reoxygenation-induced DNA damage. In a tumor, whereas regions of chronic hypoxia cells eventually die and undergo necrosis, replication restart in regions acutely subjected to low oxygen could potentially lead to an accumulation of unrepaired lesions and increased genomic instability (15). This is further aggravated by hypoxia-dependent decreased DNA repair (16). Our findings highlight the critical role of hypoxia in tumor progression and indicate that under chronic conditions, hypoxia can limit tumor progression, whereas under acute conditions, cycles of hypoxia-reoxygenation increase genomic instability.

**Authors' Affiliations:** [1]The Cancer Research UK/Medical Research Council Gray Institute for Radiation Oncology and Biology, University of Oxford, Churchill Hospital and [2]Department of Medical Oncology, University of Oxford, Weatherall Institute of Molecular Medicine, John Radcliffe Hospital, Headington, Oxford, United Kingdom

**Corresponding Author:** Ester M. Hammond, University of Oxford, Old Road Campus Research Building, Churchill Hospital, Oxford, Oxon OX3 7DQ, United Kingdom. Phone: 44-1865-617320; Fax: 44-1865-617334; E-mail: Ester.Hammond@rob.ox.ac.uk.

## Materials and Methods

**Cell lines.** RKO, HCT116, and U2OS cells were grown in DMEM with 10% FCS; IBR3 and IBR3 hTert were grown in DMEM with 15% FCS. RKO-neo and RKO-E7 lines were a gift from Dr. Kathleen Cho (University of Michigan, Ann Arbor, MI). HCT116 spheroids were grown for 15 d by adding single-cell suspensions obtained from exponential cultures to spinning flasks ($4 \times 10^6$ total cells). Pimonidazole (1 μmol/L) was added 24 h before fixation. All cell lines were *Mycoplasma*-free.

**Hypoxia treatment.** Hypoxia treatments were carried out in a Bactron II anaerobic chamber (Shell Labs) or an In vivo 400 (Ruskinn). Cells were plated on glass dishes. Acute hypoxia was considered up to 12 h whereas chronic exposure was 16 to 48 h. Where no period of reoxygenation is indicated, cells were harvested inside the chamber with equilibrated solutions.

**Fluorescence-activated cell sorting analysis.** Cells were labeled with 10 μmol/L bromodeoxyuridine (BrdUrd) (Sigma) 1 h before harvesting. Cells were processed for fluorescence-activated cell sorting (FACS) analysis on a FACSort flow cytometer (BD) after staining with mouse anti-BrdUrd antibody (BD Biosciences) and Alexa-fluor 488–conjugated goat anti-mouse IgG (Invitrogen). Quantification of cell populations was done using WinMDI 2.9 software (Scripps Research Institute).

**siRNA transfection.** p53 Silencer Select Validated siRNA (Applied Biosystems Ambion) or Stealth RNAi negative control (Invitrogen) duplexes, at a final concentration of 50 nmol/L, were transfected into RKO cells using DhamaFECT (Thermo Scientific) according to the manufacturer's instructions. 5′-3′ oligo sequence: GUAAUCUACUGGGACGGAAtt.

**DNA fiber analysis.** The DNA fiber technique was done as described recently (17), with some specific modifications (see Supplementary Fig. S2). Fiber spreads were examined using a Radiance confocal microscope (Bio-Rad). Red (CldU) and green (IdU) tracks were measured, and replication structures quantified using ImageJ software (NIH). At least 100 replication tracks were measured and 200 replication structures counted per condition per experiment.

**Immunoblotting.** Cells were lysed in UTB [9 mol/L urea, 75 mmol/L Tris-HCl (pH 7.5), and 0.15 mol/L β-mercaptoethanol] and sonicated briefly. Preparation of chromatin-bound protein extracts was done as described (18). Primary antibodies were anti-MCM6, anti-MCM7, anti-Chk1, anti-Rad51, anti-p53, and anti-actin (Santa Cruz Biotechnology); anti-RPA32 and anti-MCM5 (Dr. C. Bauerschmidt, University of Oxford, Oxford, UK); anti–proliferating cell nuclear antigen (PCNA; Calbiochem); anti–HIF-1α (BD Biosciences); anti-pATM S1981 (Epitomics); anti–pChk1 S317 (Cell Signaling Technology); and anti-TopBP1 (Abcam). Secondary antibodies were Alexa-fluor 680–conjugated goat anti-mouse and anti-rabbit IgG (Invitrogen). Detection was done using the Odyssey IR imaging technology (LI-COR Biosciences).

**Immunofluorescence.** RPA and 53BP1 staining was as described (8). ssDNA and BrdUrd staining was carried out as previously described (19). Cells were visualized using a Nikon 90i microscope or a Radiance confocal microscope (Bio-Rad).

**Immunohistochemistry.** Staining was done as described, with some modifications (20); antigen retrieval was done using EDTA (pH 8.0) for Hydroxyprobe and EDTA (pH 9.0) for CAIX and MCM6. Primary antibodies used were Hydroxyprobe (Chemicon), anti-CAIX (M75; a gift from Dr. Pastorekova, Institute of Virology, Slovak Academy of Sciences, Bratislava, Slovak Republic), and anti-MCM6 (Santa Cruz Biotechnology).

**Nucleotide quantification.** The extracts for quantification of nucleotide levels were carried in hypoxia with 3% tricarboxylic acid as described (21).

**Quantitative reverse transcription-PCR.** Quantitative real-time PCR (qRT-PCR) was done as previously described (22), using the Express SYBR GreenER qRT-PCR Supermix Kit (Invitrogen) following the manufacturer's recommendations. Reactions were carried out in a 7500 Fast Real-time PCR Detection System (Applied Biosystems). Expression levels were normalized to 18S rRNA and vascular endothelial growth factor was used as a positive control.

**Reporter assay.** Cells were transfected with the reporter constructs (80 ng/well) using Lipofectamine transfection reagent (Invitrogen), along with pCMV-Renilla (0.2 ng/well) for normalization. Firefly and Renilla luciferase activities were measured using the Dual Glo Luciferase assay (Promega).

**Statistical analysis.** The statistical significance of differences between data sets was determined assessed by using Student's *t* test. Statistical significance was assumed if $P < 0.05$ or lower and is noted in the figures. Error bars represent ±SE.

## Results

**DNA fiber analysis shows a block in replication initiation and elongation in response to severe hypoxia.** Exposure to low oxygen levels results in a rapid cessation of DNA synthesis in the absence of DNA damage (7). Oxygen levels must be below 0.1% to induce an arrest, shown by BrdUrd incorporation, and all subsequent experiments were carried out at 0% to 0.02% $O_2$ unless otherwise stated (Fig. 1A; Supplementary Fig. S1). The oxygen dependency of the arrest confirmed previous findings indicating that the S-phase arrest is independent of HIF-1 (7). The rapid cessation of DNA synthesis observed in response to severe levels of hypoxia, described here and previously, used techniques such as [³H]thymidine labeling or BrdUrd incorporation followed by FACS analysis (7, 10, 23). These methods allow the overall levels of DNA synthesis to be determined in a hypoxic cell but do not give any information about the stage of replication at which the block occurs. To fully investigate hypoxia-induced replication arrest, we have made use of the DNA fiber technique, which allows visualization of individual DNA strands and of different replication structures, as well as measurement of the speed of ongoing replication forks (Supplementary Fig. S2; ref. 24). RKO cells were exposed to hypoxia for 4, 6, or 8 hours, and the replication structures observed, quantified, and characterized as stalled forks, ongoing

forks, or new origins (Fig. 1B). It should be noted that a stalled fork could also be a first-label termination, as these two structures are indistinguishable using this technique. After 4 hours of hypoxia, the number of stalled/terminated forks increased significantly and continued to accumulate over the following 4 hours. Concomitant with the increase in stalled forks, we saw a decrease in ongoing forks. Importantly, we determined that origin firing was significantly repressed in hypoxic conditions, being nonexistent at the 8-hour time point.

We examined the rate of replication at ongoing fork speeds, measuring both the average and median rates (Fig. 1C). After 4 hours of hypoxia, the number of ongoing forks had decreased by approximately 75% and the average

and median rates of the remaining were decreased significantly when compared with normoxic samples, with a shift of the distribution severely toward the left. The fork speeds were reduced further at 6 and 8 hours of hypoxic exposure, being more than 15-fold reduced at the later time point when compared with normoxic forks (0.05 versus 0.83 kb/min median rates; Fig. 1C and data not shown). Many of the hypoxic ongoing forks have a barely detectable level of second label, leading us to consider that they are not truly representative of ongoing forks and that replication may be completely abrogated in these conditions. These data show that DNA replication is blocked at both the initiation and elongation phases in response to hypoxia.
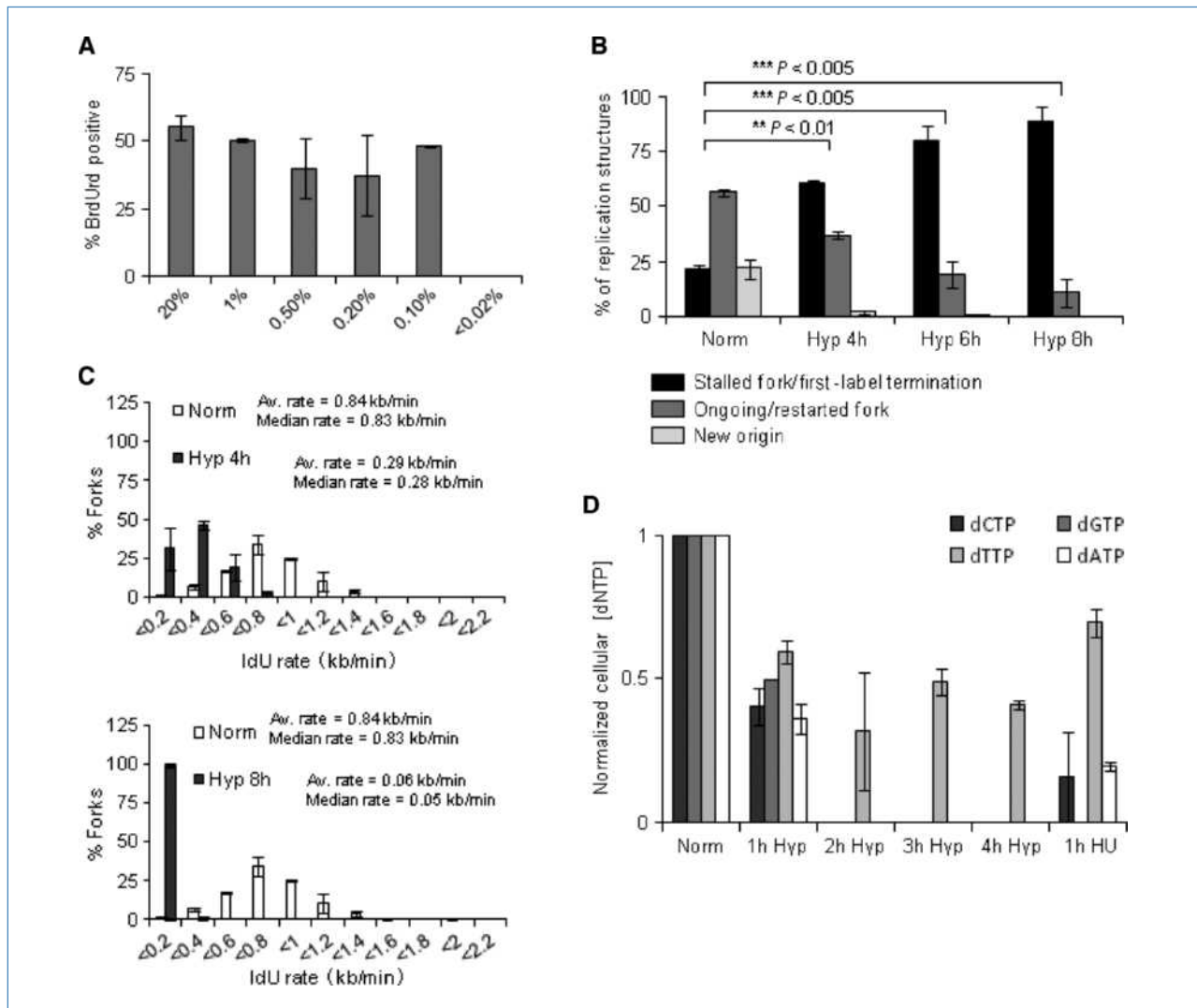


**Figure 1.** Hypoxia induces an S-phase replication arrest. Hypoxia levels $pO_2$ <0.02, unless as indicated in A. A, RKO cells were exposed to decreasing oxygen tensions for 8 h and labeled with BrdUrd. At least 200 cells were counted. B, RKO cells were exposed to hypoxia for the time points indicated and DNA fibers were produced and scored. C, graphs represent the distribution of the fork rates for the second label [iododeoxyuridine (IdU)] for the ongoing forks scored in B in normoxia (white) and hypoxia (gray) for the various hypoxic exposures. Inset, average and median fork rate values. D, HCT116 cells were exposed to hypoxia for up to 4 h or to hydroxyurea (*HU*; 2 mmol/L) for 1 h and processed to determine dNTP levels as described. Graph represents fold changes of dNTPs comparing to normoxia.
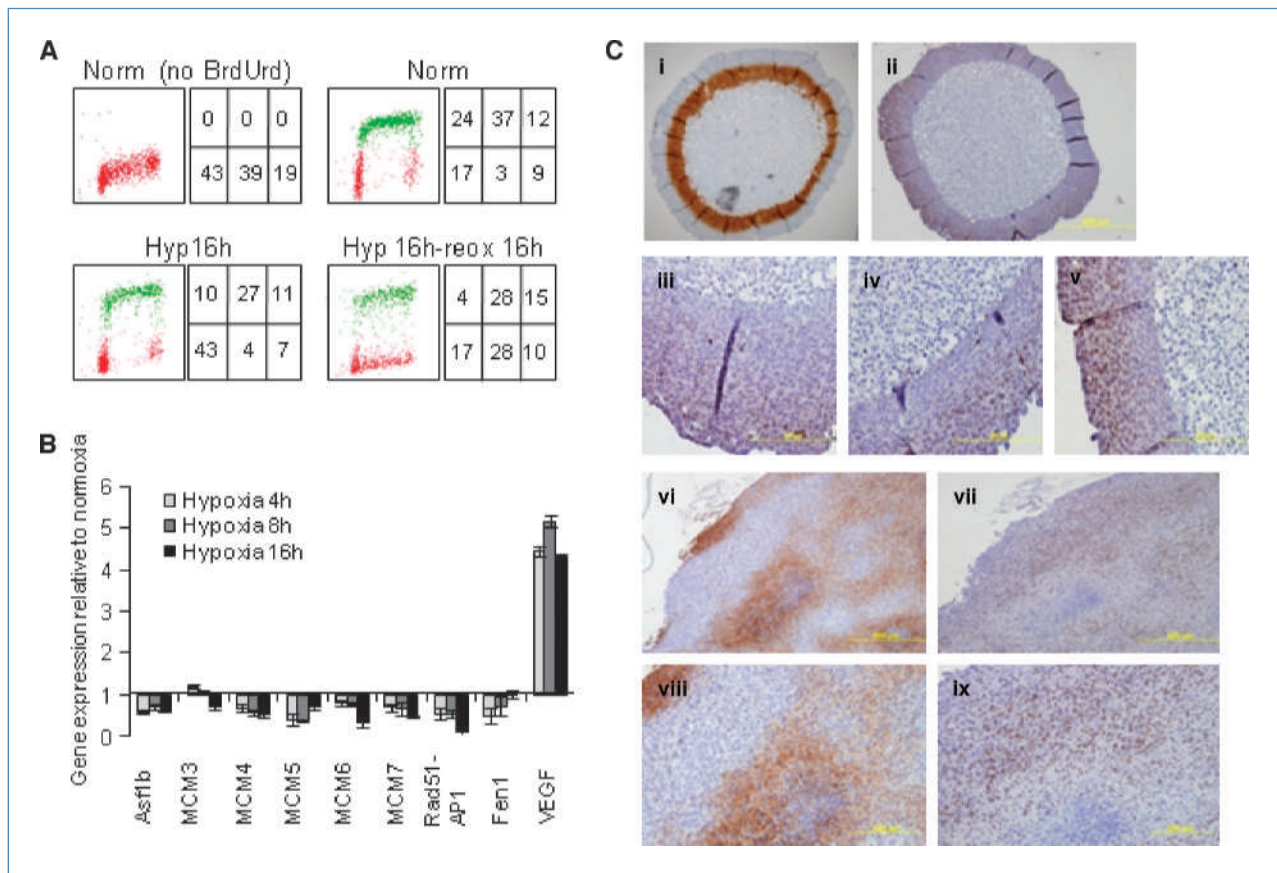
**Figure 2.** Chronic exposures to hypoxia impair replication restart after reoxygenation. Hypoxia levels $pO_2$ <0.02. A, RKO cells were pulse labeled with BrdUrd for 1 h in normoxic conditions and then harvested or exposed to hypoxia (16 h) or reoxygenation (16 h). BrdUrd-negative populations are represented in red, and BrdUrd-positive populations in green. Percentages of different cellular populations were calculated (clockwise from top left: BrdUrd positive $G_1$, BrdUrd positive S, BrdUrd positive $G_2$-M, BrdUrd negative $G_1$, BrdUrd negative S, BrdUrd negative $G_2$-M). B, replication- and repair-related genes are downregulated in hypoxia, as determined by qRT-PCR. Graph represents gene expression changes relative to normoxia. C, spheroids were stained for pimonidazole and (i) MCM6. (ii–v) U87 xenograft tumors treated with bevacizumab were stained for CAIX (vi and viii) and MCM6 (vii and ix). Scale bars are indicated. Note that viii and ix are higher magnifications of the area shown in vi and vii, respectively.

The ability of ribonucleotide reductase (RNR) to synthesize the four deoxynucleotide triphosphates (dNTP) required for DNA replication is dependent on a tyrosyl free radical within the enzymes active site. This free radical is generated in an oxygen-dependent manner and is therefore compromised under hypoxic conditions (7, 23, 25). The ability of RNR to synthesize the four dNTPs required for DNA replication is dependent on a tyrosyl free radical within the enzymes active site. This free radical is generated in an oxygen-dependent manner and is therefore compromised under hypoxic conditions (25). Nucleotide levels were measured by high-performance liquid chromatography with spectrophotometric detection in HCT116 cells exposed to hypoxia or to hydroxyurea as a control (Fig. 1D). Levels of dNTPs decreased significantly (within 1 hour) in response to hypoxia, suggesting that a loss of RNR activity under hypoxic conditions could be the underlying cause or contribute to the hypoxia-induced arrest. Significantly, dNTP levels did not decrease during exposure to milder hypoxia (2% $O_2$), which does not induce replication arrest (data not shown). The absolute

levels of RNR protein were not found to change throughout the experiment (data not shown). We also noted that energy charge was not altered during the first 24 hours of hypoxic treatment, indicating that decreased energy levels did not contribute to the arrest (Supplementary Fig. S3). This suggests a model whereby stalled forks arise during exposure to hypoxia as a result of reduced levels of dNTPs and trigger signaling pathways that inhibit origin firing, which is also reinforced by a lack of available nucleotides.

***Replication restart is inhibited in response to chronic hypoxia.*** The fate of hypoxia-arrested cells after reoxygenation is significant because reoxygenation induces significant levels of damage and major DNA repair pathways including homologous recombination are inhibited during hypoxia/reoxygenation (9, 16, 26). To investigate replication restart in this scenario, we pulse labeled RKO cells with BrdUrd to follow S-phase cells through hypoxia and reoxygenation; cells were scored as being unlabeled or labeled in the $G_1$, S, or $G_2$ phase (Fig. 2A). Labeled S-phase cells exposed to hypoxia (16 hours) failed to progress into $G_2$ after reoxygenation,

suggesting that they were replication incompetent. Unlabeled $G_1$ cells were able to progress through to S phase after reoxygenation, suggesting that the hypoxia-induced $G_1$ arrest is not permanent and that the cells were viable (27). These data indicate that chronic (16-hour) hypoxia exposure compromises the ability of the S-phase arrested cells to restart DNA replication.

Previous microarray analysis in mouse embryonic fibroblasts suggested that a number of genes involved in DNA replication or repair were repressed in hypoxic conditions, including *Asf1b, MCM3, MCM4, MCM5, MCM6, MCM7, Rad51 AP1*, and *Fen1* (22). In addition, polysomes were fractionated after 24 or 48 hours of hypoxia followed by qRT-PCR to identify gene products actively repressed in hypoxic conditions (data not shown). Of the previously identified genes,
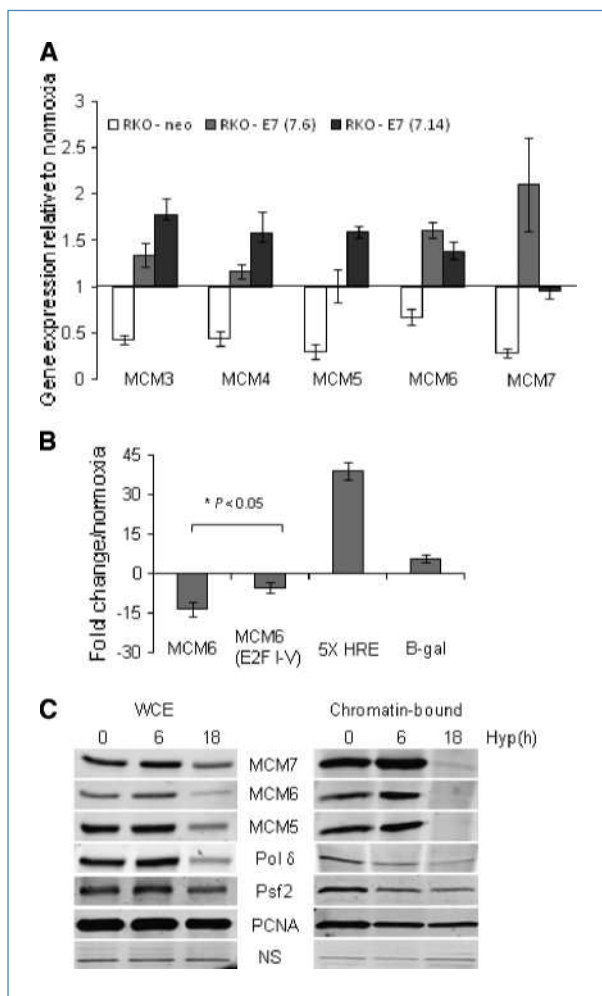


**Figure 3.** Chronic hypoxia leads to replisome disassembly. Hypoxia levels $pO_2$ <0.02. A, MCM gene expression repression is abrogated in E7-expressing RKO cells. Graph represents gene expression changes after 16-h hypoxia relative to normoxia. B, normalized luciferase activity (firefly/Renilla) fold change for 16-h hypoxia relative to normoxic controls for MCM6 promoter and respective E2F binding site mutant. C, chromatin fractions and whole-cell extracts for MCM5, MCM6, MCM7, and PCNA protein levels in normoxia and hypoxia for HCT116 cells. NS, nonspecific band.

*MCM3, MCM4, MCM5*, and *Asf1b* were found to be repressed. We have verified by qRT-PCR the repression of components of the replication machinery under hypoxic conditions in a human cell line (Fig. 2B). Before proceeding further, we determined if hypoxia downregulation of key replication factors occurred both at the protein level and *in vivo*. The MCM complex (MCM2–MCM7) is loaded onto the chromatin in the $G_1$ cell cycle phase to form the pre-replicative complexes, and their helicase function is activated on initiation and required for duplex unwinding during ongoing replication (28, 29). First, the HCT116 cell line was grown as spheroids before staining for MCM6 and the hypoxia marker pimonidazole (Fig. 2C, i–v). The outer layers of the spheroids show a strong nuclear stain of MCM6, whereas the cells surrounding the necrotic core show no or greatly reduced levels of MCM6. As expected, the pattern of pimonidazole staining is inverse to that seen for MCM6, that is, more positive toward the necrotic core, indicating increasing levels of hypoxia. U87 cells were grown as xenograft tumors and treated with the antiangiogenic agent bevacizumab (30). The tumors were sectioned and stained for CAIX and MCM6 (Fig. 2C, vi–ix). As expected, viable cells within CAIX-positive regions showed decreased levels of MCM6. In both models, we noticed that MCM6 levels decrease before cells become obviously necrotic, supporting our hypothesis that this is an active mechanism induced in response to hypoxia and not a result of cell death. It should be noted than in both systems, additional microenvironmental stresses not present in *in vitro* experiments may also play a role in the repression of MCM6, for example, nutrient deprivation (glucose and amino acids) and acidosis.

The E2F transcription factors have been shown to be important for the cell growth–regulated expression of the MCM proteins as well as for the repression of DNA repair during hypoxia (31, 32). We investigated whether the hypoxia-induced repression of MCM proteins is E2F dependent, first, by using the overexpression of human papillomavirus (HPV) E7. HPV E7 disrupts the E2F/pocket protein interaction and also targets pocket proteins for degradation, thus interfering with E2F activity (31). The expression levels of MCM3 to MCM7 were compared in two RKO cell lines overexpressing E7 with a matched control (Fig. 3A). In each case, the hypoxia-induced repression was significantly alleviated by the presence of E7. To validate the involvement of the E2Fs, we made use of a *MCM6* reporter construct with all the identified E2F binding sites mutated (32). In response to hypoxia, we observed a 10- to 20-fold repression of the *MCM6* promoter in contrast to a 5× HRE luciferase construct, which was induced 40-fold (Fig. 3B). Loss of E2F binding significantly altered the repression of *MCM6* in response to hypoxia.

Our next step was to examine what effect the repression of the *MCM* mRNAs had on the protein levels of MCM5, MCM6, and MCM7 (Fig. 3C). In each case, the protein levels decreased and most significantly so after more chronic hypoxia exposures, and it should be noted that this was not due to a loss of S-phase cells (Fig. 2A). Because the protein levels for the MCMs were not completely abrogated, potentially due to the long half-life of these proteins (24 hours; ref. 33), we investigated whether the remaining MCM proteins
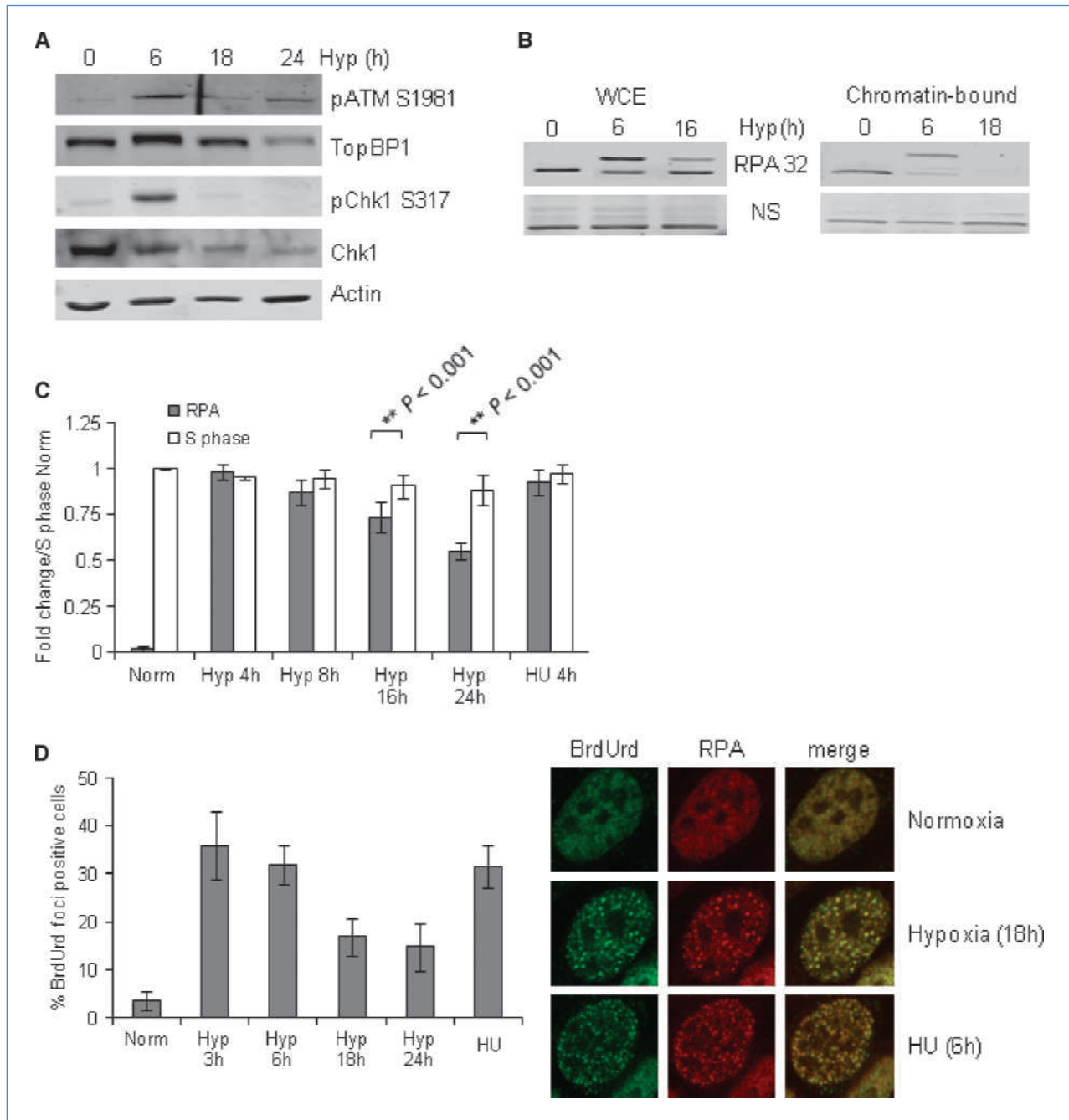
**Figure 4.** DNA damage response is inhibited after chronic exposures to hypoxia. Hypoxia levels $pO_2$ <0.02. A, representative Western blots showing pATM S1981, TopBP1, Chk1, and pChk1 S317 levels for normoxia and hypoxia for HCT116 cells. B, Western blots for chromatin fractions and whole-cell extracts for RPA protein levels, as in Fig. 3C. C, RKO cells were pulse labeled with BrdUrd for 1 h in normoxic conditions or exposed to hypoxia or to hydroxyurea for 4 h. Data represent the fold change relative to normoxia of RPA foci–positive (gray) and BrdUrd-positive (white) cells of total cell number. D, BrdUrd-labeled RKO cells exposed to hypoxia or to hydroxyurea for 6 h (19). Cells were then costained for BrdUrd and RPA. Data represent the number of ssDNA (BrdUrd)-positive cells. At least 200 cells were counted per slide.

were functional by determining their cellular location. Extraction of chromatin-bound proteins after chronic exposure to hypoxia showed no association of MCM5, MCM6, or MCM7 with the chromatin, indicating a complete lack of replisome function (Fig. 3C). The GINS proteins have been shown to in-

teract with the MCMs and are essential for DNA replication (34). We investigated one of the GINS proteins, Psf2, and found that total levels of Psf2 decreased rapidly in hypoxia. We have also shown that, as predicted by the polysome assay, levels of polymerase δ are repressed in hypoxic conditions and show

decreased chromatin association. This was not a general effect because PCNA remained chromatin bound during both acute and chronic hypoxia. Taken together, these data indicate that replication does not resume after chronic periods of hypoxia due to an active disassembly of the replisome including both the helicases and polymerases. The mechanism behind this seems to be multifactorial. These data are supportive of a transcriptional model in which activating E2Fs are replaced on the *MCM6* promoter with repressive E2Fs, possibly E2F4 because it is the most sensitive to E7 expression during hypoxia exposure (35). In addition, the MCM complex is not retained at the replication fork potentially due to a loss of interacting factors such as Psf2. The MCM complex has been shown to be phosphorylated by ATM and ATR in re-

sponse to replication stress (MCM2 and MCM3), whereas MCM7 has been shown to interact with ATR-interacting protein (36). Both the ATM and ATR kinases have been shown to be active during hypoxia, and it is therefore plausible that they contribute to MCM/replisome stability.

The accumulation of stalled replication forks or replicative stress has been shown to activate the DDR. Acute hypoxia exposure induced both ATM-S1981 and Chk1-S317, indicating the activity of both the ATM and ATR kinases. However, these signals were lost or decreased with increasing hypoxia exposure time (Fig. 4A). An integral step in the DDR to replication stress is the recognition of regions of ssDNA at stalled forks and binding of RPA. The levels of RPA did not change during hypoxia although there was a robust



Figure 5. Reoxygenation-induced replication restart occurs after acute hypoxia exposure. Hypoxia levels $pO_2$ <0.02. A, chase experiment as described in Fig. 2A. B, RKO cells were exposed to 6-h hypoxia and reoxygenated for 1 h and DNA fibers were produced. DNA fibers were also prepared under normoxic (*norm*) conditions. C, dNTP levels of RKO cells exposed to hypoxia up to 6 h and after 2-h reoxygenation. Average replication fork speeds are indicated.
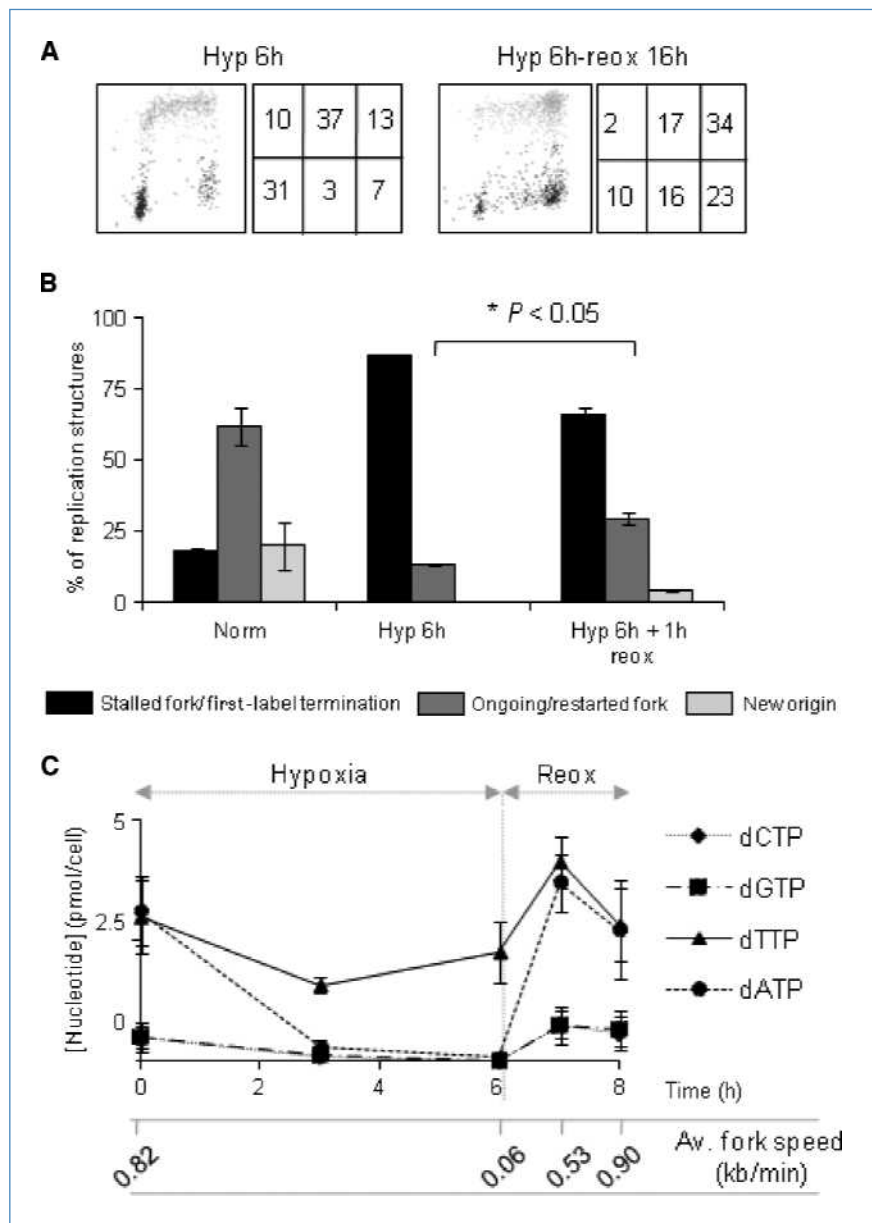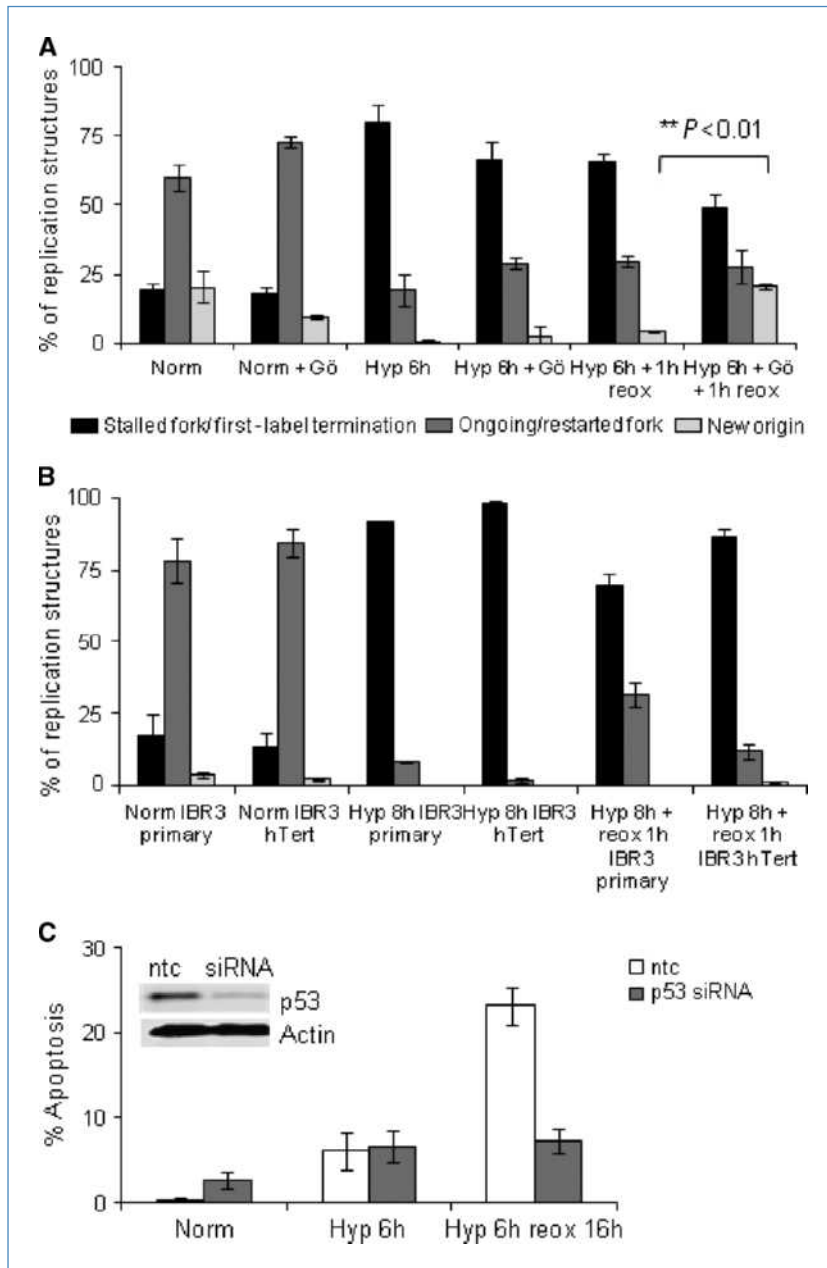
**Figure 6.** Characterization of reoxygenation-induced replication restart after acute hypoxia exposure. Hypoxia levels $pO_2$ <0.02. A, RKO cells, in the presence of either vehicle alone or 100 nmol/L of the Chk1 inhibitor Gö6976, were exposed to 6-h hypoxia and reoxygenated for 1 h and DNA fibers were produced. B, IBR3 primary and hTert immortalized fibroblasts were exposed to 8-h hypoxia and reoxygenated for 1 h, and DNA fibers produced. C, RKO cells were transfected with either nontargeting siRNA control (*ntc*) or p53 siRNA and the knockdown was validated by Western blotting. Apoptosis levels were determined by scoring cells with characteristic nuclear morphology after 4′,6-diamidino-2-phenylindole staining. At least 200 cells were scored per sample.

ATM-dependent phosphorylation during acute exposure that was absent after longer times (Fig. 4B; Supplementary Fig. S4A and B). RPA was found to be chromatin associated during acute, but not chronic, hypoxia. In support of this, we found that RPA formed clear nuclear foci in response to hypoxia but that these decreased as exposure time increased (Fig. 4C). We then verified that the hypoxia-induced RPA foci were indeed regions of ssDNA by costaining for BrdUrd in labeled but nondenatured cells. The RPA foci and regions of ssDNA completely colocalized (Fig. 4D). This prompted us to count the number of cells positive for ssDNA by BrdUrd staining. We found that this signal also decreases with increasing exposure time, indicating that the signal which

initiates the DDR in response to hypoxia decreases after extended periods, potentially due to slow or residual polymerase activity (37). These data are supportive of the hypoxia-induced DDR stabilizing the replisome during acute exposure, potentially through phosphorylation of the MCM complex, although we have not been able to verify this.

***Cells exposed to acute hypoxia/reoxygenation remain replication competent.*** In response to chronic exposure to hypoxia, essential components of both the replication machinery and the DDR are repressed, which together lead to the destabilization of the replication fork and prevent subsequent restart. However, closer examination of our data indicates that this may not be the case during shorter/acute

exposures (less than 12 hours). This raises the possibility that cells that have undergone hypoxia-induced replication arrest for shorter time periods might be capable of replication restart. To address this, we repeated the BrdUrd chase experiment and found that labeled S-phase cells indeed progressed through the cell cycle to $G_2$ (Fig. 5A). To investigate this further, we have again made use of the DNA fiber technique. After acute exposure to hypoxia (6 hours), followed by reoxygenation, there was a significant increase in the number of ongoing forks, an increase in the number of new origins, and, as expected, a decrease in the number of stalled forks (Fig. 5B). Using the mitotic shake-off technique, we have ruled out any contribution of hypoxic $G_1$ cells entering S phase during reoxygenation in the fiber analysis (Supplementary Fig. S5A). Our data suggest that hypoxia-induced replication arrest is dependent on a decrease in dNTPs (Fig. 1D); here, we investigated the dNTP levels after reoxygenation. As previously, we saw a rapid and significant drop in all four nucleotides in response to hypoxia; however, these levels returned to normal within 2 hours of reoxygenation (Fig. 5C). The same trend was also seen in HCT116 cells (data not shown). Interestingly, we found that this correlated with reoxygenation-restarted replicating fork rates, which were slower than those under normoxic conditions but returned to normal within 2 hours after reoxygenation (Fig. 5C). Despite reoxygenation-induced damage and activation of the ATM/ATR signaling pathways, DNA replication resumes during reoxygenation after acute hypoxia.

In addition to its role in regulating initiation and elongation in unperturbed cells, Chk1 has been shown to regulate these processes following replication stress such as UV, camptothecin, and hydroxyurea (18, 38–40). However, the role of Chk1 in hypoxia-mediated arrest and reoxygenation-induced restart is unknown. Pharmacologic inhibition of Chk1 by treatment with Gö6976 did not significantly change the number of ongoing forks, suggesting that Chk1 did not affect the hypoxia-induced arrest (Fig. 6A). Chk1 inhibition led to an overall decrease in average and median speed even in the absence of hypoxic stress, which was not further exacerbated by hypoxia exposure (data not shown). During replication restart after acute hypoxia, however, loss of Chk1 led to a significant increase in the number of new origins firing. This is supported by previous data indicating a role for Chk1 in mediating the S-phase checkpoint (41, 42). Again, this was verified using the mitotic shake-off technique (Supplementary Fig. S5A).

We have considered that replication restart might be restricted to tumor cell lines or possibly cells deficient in mismatch repair as used here and have therefore investigated this after reoxygenation in a nontransformed cell line (43). Primary 1BR3 and immortalized 1BR3 hTert cell lines were exposed to hypoxia and reoxygenation (Fig. 6B). In both cases, cells arrested in response to hypoxia as determined by a significant increase in the number of stalled/terminated forks. In both cases, Chk1 was also phosphorylated during hypoxia exposure (data not shown). Reoxygenation-induced replication restart was measured in both cell lines and seemed to be slightly more robust in the 1BR3 compared with the 1BR3 hTert line.

These data show that replication restart is not restricted to transformed cell lines after reoxygenation but is a more widespread phenomenon.

These findings led us to hypothesize that, to prevent reoxygenated cells undergoing replication restart from contributing to genomic instability, cell death might be induced. RKO cells were treated with siRNA to p53 or a nontargeting control followed by 6 hours of hypoxia and reoxygenation, and the levels of apoptosis were then determined (Fig. 6C). The p53 status did not affect the level of hypoxia-induced apoptosis, which was approximately 5%. However, after reoxygenation, there was a significant increase in apoptosis, which was p53 dependent. These data indicate that p53-proficient cells that undergo replication restart should be eradicated from the tumor population by apoptosis, whereas those that have p53-pathway mutations escape and contribute to genomic instability.

## Discussion

We have conclusively shown that replication is abrogated in hypoxic conditions during both the initiation and elongation phases and that this correlates with decreasing dNTP levels potentially resulting from decreased RNR activity. Until now, it has been unclear whether cells exposed to hypoxia-induced replication arrest are capable of completing S phase after a reoxygenation event. Our data show that this is critically dependent on the exposure time to hypoxia.

Even when still viable, chronically arrested cells are incapable of replication restart in response to reoxygenation and therefore do not contribute to continued tumorigenesis. We have attributed this to a complete loss of replisome stability as well as hypoxia-mediated downregulation of the homologous recombination pathway. In contrast, our data show that after shorter periods of hypoxia-induced replication arrest, cells are able to resume replication in response to reoxygenation. Importantly, this occurs in the presence of reactive oxygen species–induced DNA damage and when essential DNA repair pathways are somewhat inhibited, including nonhomologous end joining, mismatch repair, and homologous recombination (16, 26). A number of genes essential to these repair pathways have been identified that are specifically repressed during hypoxia, including *Rad51, Rad52, BRCA1, BRCA2, Ku70, DNA-PKcs, LigIV, MLH1, MSH2,* and *MSH6* (44–48). Together, these data indicate that cells that resume DNA synthesis after a reoxygenating event do so in the presence of DNA damage and with impaired DNA repair capabilities. Our data show that if these restarted cells retain p53 activity, they undergo apoptosis. However, because the majority of tumor cells harbor p53 or p53-pathway mutations, it is more likely that cycling through periods of acute hypoxia followed by reoxygenation will lead to an accumulation of unrepaired lesions and increased genomic instability (15). Encouragingly, our findings indicate that therapeutic options, such as bevacizumab, may enhance the potential effects of DNA repair/replication inhibitors and therefore suggest that a combined approach may be an effective way to target hypoxic regions. In addition, these findings suggest

that combining repair/replication inhibitors with therapies with vascular normalization properties may effectively target cells undergoing reoxygenation-induced replication restart.

## Disclosure of Potential Conflicts of Interest

## Acknowledgments

## Grant Support

## References

1. Hockel M, Vaupel P. Tumor hypoxia: definitions and current clinical, biologic, and molecular aspects. J Natl Cancer Inst 2001;93:266–76.
2. Erler JT, Bennewith KL, Nicolau M, et al. Lysyl oxidase is essential for hypoxia-induced metastasis. Nature 2006;440:1222–6.
3. Brown JM, Wilson WR. Exploiting tumour hypoxia in cancer treatment. Nat Rev Cancer 2004;4:437–47.
4. Cardenas-Navia LI, Mace D, Richardson RA, Wilson DF, Shan S, Dewhirst MW. The pervasive presence of fluctuating oxygenation in tumors. Cancer Res 2008;68:5812–9.
5. Brown JM. Tumor hypoxia in cancer therapy. Methods Enzymol 2007;435:297–321.
6. Hammond EM, Denko NC, Dorie MJ, Abraham RT, Giaccia AJ. Hypoxia links ATR and p53 through replication arrest. Mol Cell Biol 2002;22:1834–43.
7. Hammond EM, Green SL, Giaccia AJ. Comparison of hypoxia-induced replication arrest with hydroxyurea and aphidicolin-induced arrest. Mutat Res 2003;532:205–13.
8. Bencokova Z, Kaufmann MR, Pires IM, Lecane PS, Giaccia AJ, Hammond EM. ATM activation and signaling under hypoxic conditions. Mol Cell Biol 2009;29:526–37.
9. Hammond EM, Dorie MJ, Giaccia AJ. ATR/ATM targets are phosphorylated by ATR in response to hypoxia and ATM in response to reoxygenation. J Biol Chem 2003;278:12207–13.
10. Freiberg RA, Hammond EM, Dorie MJ, Welford SM, Giaccia AJ. DNA damage during reoxygenation elicits a Chk2-dependent checkpoint response. Mol Cell Biol 2006;26:1598–609.
11. Gibson SL, Bindra RS, Glazer PM. Hypoxia-induced phosphorylation of Chk2 in an ataxia telangiectasia mutated-dependent manner. Cancer Res 2005;65:10734–41.
12. Bartkova J, Horejsi Z, Koed K, et al. DNA damage response as a candidate anti-cancer barrier in early human tumorigenesis. Nature 2005;434:864–70.
13. Gorgoulis VG, Vassiliou LV, Karakaidos P, et al. Activation of the DNA damage checkpoint and genomic instability in human precancerous lesions. Nature 2005;434:907–13.
14. Hammond EM, Kaufmann MR, Giaccia AJ. Oxygen sensing and the DNA-damage response. Curr Opin Cell Biol 2007;19:680–4.
15. Aguilera A, Gomez-Gonzalez B. Genome instability: a mechanistic view of its causes and consequences. Nat Rev Genet 2008;9:204–17.
16. Bindra RS, Crosby ME, Glazer PM. Regulation of DNA repair in hypoxic cancer cells. Cancer Metastasis Rev 2007;26:249–60.
17. Bryant HE, Petermann E, Schultz N, et al. PARP is activated at stalled forks to mediate Mre11-dependent replication restart and recombination. EMBO J 2009;28:2601–15.
18. Syljuasen RG, Sorensen CS, Hansen LT, et al. Inhibition of human Chk1 causes increased initiation of DNA replication, phosphorylation of ATR targets, and DNA breakage. Mol Cell Biol 2005;25:3553–62.
19. Hammond EM, Dorie MJ, Giaccia AJ. Inhibition of ATR leads to increased sensitivity to hypoxia/reoxygenation. Cancer Res 2004;64:6556–62.
20. Generali D, Berruti A, Brizzi MP, et al. Hypoxia-inducible factor-1α expression predicts a poor response to primary chemoendocrine therapy and disease-free survival in primary human breast cancer. Clin Cancer Res 2006;12:4562–8.
21. Decosterd LA, Cottin E, Chen X, et al. Simultaneous determination of deoxyribonucleoside in the presence of ribonucleoside triphosphates in human carcinoma cells by high-performance liquid chromatography. Anal Biochem 1999;270:59–68.
22. Hammond EM, Mandell DJ, Salim A, et al. Genome-wide analysis of p53 under hypoxic conditions. Mol Cell Biol 2006;26:3492–504.
23. Probst G, Riedinger HJ, Martin P, Engelcke M, Probst H. Fast control of DNA replication in response to hypoxia and to inhibited protein synthesis in CCRF-CEM and HeLa cells. Biol Chem 1999;380:1371–82.
24. Wilsker D, Petermann E, Helleday T, Bunz F. Essential function of Chk1 can be uncoupled from DNA damage checkpoint and replication control. Proc Natl Acad Sci U S A 2008;105:20752–7.
25. Nordlund P, Reichard P. Ribonucleotide reductases. Annu Rev Biochem 2006;75:681–706.
26. Huang LE, Bindra RS, Glazer PM, Harris AL. Hypoxia-induced genetic instability—a calculated mechanism underlying tumor progression. J Mol Med 2007;85:139–48.
27. Green SL, Freiberg RA, Giaccia AJ. p21(Cip1) and p27(Kip1) regulate cell cycle reentry after hypoxic stress but are not necessary for hypoxia-induced arrest. Mol Cell Biol 2001;21:1196–206.
28. Diffley JF. Regulation of early events in chromosome replication. Curr Biol 2004;14:R778–86.
29. Pacek M, Walter JC. A requirement for MCM7 and Cdc45 in chromosome unwinding during eukaryotic DNA replication. EMBO J 2004;23:3667–76.
30. Li JL, Sainson RC, Shi W, et al. Delta-like 4 Notch ligand regulates tumor angiogenesis, improves tumor vascular function, and promotes tumor growth in vivo. Cancer Res 2007;67:11244–53.
31. Bindra RS, Gibson SL, Meng A, et al. Hypoxia-induced downregulation of BRCA1 expression by E2Fs. Cancer Res 2005;65:11597–604.
32. Ohtani K, Iwanaga R, Nakamura M, et al. Cell growth-regulated expression of mammalian MCM5 and MCM6 genes mediated by the transcription factor E2F. Oncogene 1999;18:2299–309.
33. Guida T, Salvatore G, Faviana P, et al. Mitogenic effects of the up-regulation of minichromosome maintenance proteins in anaplastic thyroid carcinoma. J Clin Endocrinol Metab 2005;90:4703–9.
34. Aparicio T, Guillou E, Coloma J, Montoya G, Mendez J. The human GINS complex associates with Cdc45 and MCM and is essential for DNA replication. Nucleic Acids Res 2009;37:2087–95.
35. Attwooll C, Lazzerini Denchi E, Helin K. The E2F family: specific functions and overlapping interests. EMBO J 2004;23:4709–16.
36. Cortez D, Glick G, Elledge SJ. Minichromosome maintenance proteins are direct targets of the ATM and ATR checkpoint kinases. Proc Natl Acad Sci U S A 2004;101:10078–83.
37. Vassin VM, Anantha RW, Sokolova E, Kanner S, Borowiec JA.

Human RPA phosphorylation by ATR stimulates DNA synthesis and prevents ssDNA accumulation during DNA-replication stress. J Cell Sci 2009.

38. Maya-Mendoza A, Petermann E, Gillespie DA, Caldecott KW, Jackson DA. Chk1 regulates the density of active replication origins during the vertebrate S phase. EMBO J 2007;26:2719–31.

39. Petermann E, Maya-Mendoza A, Zachos G, Gillespie DA, Jackson DA, Caldecott KW. Chk1 requirement for high global rates of replication fork progression during normal vertebrate S phase. Mol Cell Biol 2006;26:3319–26.

40. Scorah J, McGowan CH. Claspin and Chk1 regulate replication fork stability by different mechanisms. Cell Cycle 2009;8.

41. Sorensen CS, Syljuasen RG, Falck J, et al. Chk1 regulates the S phase checkpoint by coupling the physiological turnover and ionizing radiation-induced accelerated proteolysis of Cdc25A. Cancer Cell 2003;3:247–58.

42. Heffernan TP, Simpson DA, Frank AR, et al. An ATR- and Chk1-dependent S checkpoint inhibits replicon initiation following UVC-induced DNA damage. Mol Cell Biol 2002;22:8552–61.

43. Kondo A, Safaei R, Mishima M, Niedner H, Lin X, Howell SB. Hypoxia-induced enrichment and mutagenesis of cells that have lost DNA mismatch repair. Cancer Res 2001;61:7603–7.

44. Bindra RS, Schaffer PJ, Meng A, et al. Down-regulation of Rad51 and decreased homologous recombination in hypoxic cancer cells. Mol Cell Biol 2004;24:8504–18.

45. Chan N, Koritzinsky M, Zhao H, et al. Chronic hypoxia decreases synthesis of homologous recombination proteins to offset chemoresistance and radioresistance. Cancer Res 2008; 68:605–14.

46. Meng AX, Jalali F, Cuddihy A, et al. Hypoxia down-regulates DNA double strand break repair gene expression in prostate cancer cells. Radiother Oncol 2005;76:168–76.

47. Koshiji M, To KK, Hammer S, et al. HIF-1α induces genetic instability by transcriptionally downregulating MutSα expression. Mol Cell 2005;17:793–803.

48. Mihaylova VT, Bindra RS, Yuan J, et al. Decreased expression of the DNA mismatch repair gene Mlh1 under hypoxic stress in mammalian cells. Mol Cell Biol 2003;23:3265–73.